

Accepted Manuscript

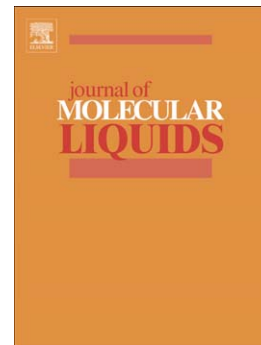
Synthesis, characterization and liquid crystalline properties of a series of hydroxybiphenyl benzoate and biphenyl bis(benzoate)

Salhed Ahmed, Md. Mostafizur Rahman, Ashikur Rahman Rabbi, Md. Kausar Ahmed, S.M. Saiful Islam, Muhammad Younus, Bimal Bhusan Chakraborty, Sudip Choudhury, Shamim Ahmed, Nasim Sultana

PII: S0167-7322(16)31959-6
DOI: doi:[10.1016/j.molliq.2016.10.002](https://doi.org/10.1016/j.molliq.2016.10.002)
Reference: MOLLIQ 6406

To appear in: *Journal of Molecular Liquids*

Received date: 19 July 2016
Accepted date: 1 October 2016



Please cite this article as: Salhed Ahmed, Md. Mostafizur Rahman, Ashikur Rahman Rabbi, Md. Kausar Ahmed, S.M. Saiful Islam, Muhammad Younus, Bimal Bhusan Chakraborty, Sudip Choudhury, Shamim Ahmed, Nasim Sultana, Synthesis, characterization and liquid crystalline properties of a series of hydroxybiphenyl benzoate and biphenyl bis(benzoate), *Journal of Molecular Liquids* (2016), doi:[10.1016/j.molliq.2016.10.002](https://doi.org/10.1016/j.molliq.2016.10.002)

This is a PDF file of an unedited manuscript that has been accepted for publication. As a service to our customers we are providing this early version of the manuscript. The manuscript will undergo copyediting, typesetting, and review of the resulting proof before it is published in its final form. Please note that during the production process errors may be discovered which could affect the content, and all legal disclaimers that apply to the journal pertain.

Synthesis, characterization and liquid crystalline properties of a series of hydroxybiphenyl benzoate and biphenyl bis(benzoate)

Salhed Ahmed^a, Md. Mostafizur Rahman^a, Ashikur Rahman Rabbi^a, Md. Kausar Ahmed^a, S.M. Saiful Islam^a, Muhammad Younus^{a*}, Bimal Bhusan Chakraborty^b, Sudip Choudhury^b, Shamim Ahmed^c, Nasim Sultana^c

^a Department of Chemistry, Shahjalal University of Science and Technology, Sylhet-3114, Bangladesh; ^b Department of Chemistry, Assam University, Silchar, India; ^c Bangladesh Council of Scientific and Industrial Research, Dhaka 1000, Bangladesh.

* Corresponding Author. E-mail: myouns-che@sust.edu

Abstract

Two series of hydroxybiphenyl benzoate **2a-2c** and biphenyl bis(benzoate) **3a-3c** have been synthesized by the esterification reaction of 4-alkoxybenzoic acid **1a-1c** with 1,1'-biphenyl-4,4'-diol in presence of DCC and DMAP in dichloromethane at room temperature under nitrogen atmosphere. Products ratio (**2** vs **3**) were not significantly influenced with the variation of alkoxy substituents. The newly synthesized ester products were characterized by IR and NMR spectroscopy as well as elemental analysis. The transition temperatures and mesophases have been investigated by differential scanning calorimetry and polarized optical microscopy. Although the synthesized ester derivatives, **3a-c** are achiral, molecular chirality is exhibited in their mesophases.

Key words: Biphenyl benzoate; liquid crystals; achiral; chiral

1. Introduction

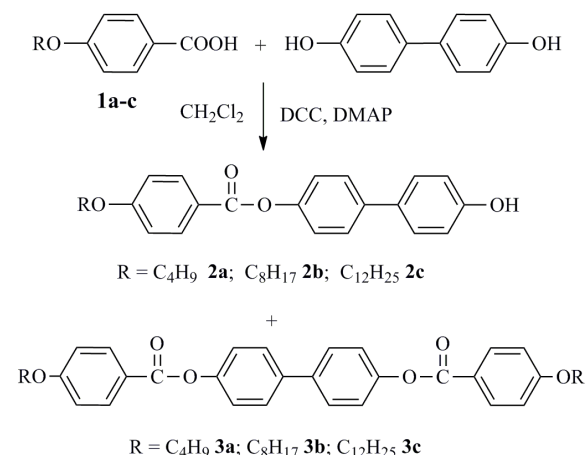
Thermochromism is a well-known and useful property frequently observed in different types of materials [1]. The change of color with temperature is certainly a phenomenon which is of interest in the field of liquid crystals [2], and many applications are based on this property: thermometers (fever indicator and gadgets), colored electro optic films and light-emitting diodes [3]. Phototunability of the cholesteric liquid crystals pitch and the circular polarized reflection wavelength has formed the basis of many applications including tunable color reflectors and filters, sensors, tunable lasers and molecular switches [4-12]. Chirality is a very intriguing issue in liquid crystal (LC) science [13]. There are many types of chiral LCs, such as chiral nematic (N*) [14], chiral smectic C (SC*) [15], blue phase [16-17] and twisted grain boundary (TGB) phase [18]. Liquid crystal molecules can be made chiral either by including chirality within the molecules or by adding chiral dopant into liquid crystal phases [13, 19]. In recent years, there have been many reports on the design of liquid crystals exhibiting chiral phases, without possessing any chiral center [20-21]. Among them, bent-core molecules with one or two flexible tails exhibit a wide variety of novel structural phenomena involving the interplay of chiral, polar, and liquid crystalline order [20c-d]. During controlled heating or cooling, these materials form isotropic fluid, though they possess short range positional and orientational order. As a result, the macroscopic symmetry is broken to produce chirality, despite the fact that these molecules are achiral. This type of symmetry breaking is observed in nematic and smectic phases, and polarized optical microscopy gives regions of different optical properties. Rotation of one polarizer from its crossed position clockwise by a certain angle (< 20°) gives two different optical domains, and rotating the polarizer in the opposite direction by the same angle reverses the position of the domains. Although a vast number of achiral bent-core (1-3-substituted phenyl core)

liquid crystals with chiral phases are available in the literature [20c-d, 21], rod-like liquid crystals using biphenyl and phenylpyrimidine linked *via* flexible methylene spacer are also reported [20a-b]. In this study, we report the synthesis and characterization of a new series of hydroxybiphenyl benzoate **2a-2c** and biphenyl bis(benzoate) **3a-3c** and investigation of their liquid crystalline properties. The use of long, linear aromatic biphenyl ring contributes to the thermal stability of the mesophase. Though the newly formed ester derivatives **3a-c** are achiral, the molecular chirality is exhibited in their mesophases without introducing chiral dopants.

2. Results and discussion

2.1 Syntheses

The ester products of hydroxybiphenyl benzoate **2a**, and biphenyl bis(benzoate) **3a** were synthesized by the



Scheme 1 Synthesis of hydroxybiphenyl alkoxybenzoate and biphenyl bis(alkoxybenzoate) derivatives

Table 1 Synthesis of hydroxybiphenyl alkoxybenzoate and biphenyl bis(alkoxybenzoate) derivatives^a

Entry	4-Alkoxybenzoic acid, 1 (2.32 mmol)	1,1'-Biphenyl-4,4'-diol (mmol)	Hydroxybiphenyl alkoxybenzoate 2 , ⁱ (%)	Biphenyl bis(alkoxybenzoate) 3 , ⁱ (%)
1	1a	2.32	21.5 (2a)	18.3 (3a)
2	1b	2.32	25.5 (2b)	24.6 (3b)
3	1c	2.32	20.7 (2c)	14.2 (3c)

^a The esterification reactions were performed in DCC (2.32 mmol) and DMAP (2.32 mmol) in dry dichloromethane at room temperature.

ⁱ Isolated yields.

esterification reaction [22] of 4-butoxybenzoic acid **1a** with 1,1'-biphenyl-4,4'-diol in presence of DCC and DMAP in dichloromethane at room temperature under nitrogen atmosphere. The newly synthesized compounds **2a** and **3a** were isolated as white solids in 21.5% and 18.3% respectively (Table 1, entry 1, and Scheme 1). Using excess 1,1'-biphenyl-4,4'-diol (6 equivalent) in the reaction increases the yield of the mono-benzoate **2a** by 9% (isolated yield 30.5%), but the formation of bis-benzoate **3a** remains the same. Utilizing excess (6 equivalents) 4-butoxybenzoic acid **1a** in the reaction increases the yield of the bis-benzoate **3a** significantly (54.1 %). The synthesized ester derivatives were purified and isolated by column chromatography eluting with hexane and dichloromethane (2:1). Similarly, other ester products **2b-c**, and **3b-c** with longer carbon chains (C₈ and C₁₂) were synthesized. The synthetic route for biphenyl benzoate derivatives is shown in Scheme 1. Products ratio (**2** vs **3**) were not significantly influenced with the variation of alkoxy substituent. The results were summarized in Table 1. All the synthesized ester products provided satisfactory elemental analyses. The structure of ester products **2a-2c** and **3a-3c** were confirmed by IR, ¹H and ¹³C NMR spectroscopic techniques (Table 2). Although the preparation of compound **2a** and **2b** were reported previously, **2a** was isolated as an impure product, could not be purified by recrystallization and column chromatography [23], and characterization of **2b** was limited to IR and ¹H NMR spectroscopy [24].

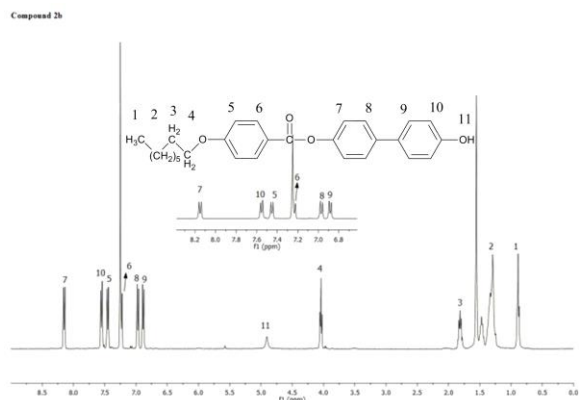
2.2. Characterization

In the IR spectra, the $\nu(\text{C}=\text{O})$ stretching frequency is diagnostic of the characterization of the ester group (-COOR), and the absence of the terminal acidic hydrogen, -COOH confirms the completion of the reaction. The ester product **2a** displays a sharp single absorption band at 1707 cm⁻¹, which is assigned to the stretching vibration of the ester group (RCOOR). The compound shows no broad band for the -COOH stretching vibration in the range of 2400-3400 cm⁻¹ confirming that the terminal carboxylic acidic group (-COOH) undergo the esterification with the hydroxyl group of 1,1'-biphenyl-4,4'-diol. The spectrum displays another single absorption band at 3458 cm⁻¹, characteristic of -OH stretching vibration, demonstrating that the esterification reaction occurs in one hydroxyl group and another hydroxyl group is retained in the compound [25]. Similarly, compound **3a** displays the presence of a sharp absorption at 1728 cm⁻¹ and absence of a broad band in the range of 2400-3400 cm⁻¹, thus confirming the formation of the desired ester product (RCOOR). Compound **2a** displays a single IR absorption band at 3458 cm⁻¹, characteristic of -OH stretching vibration, whereas compound **3a** does not display any absorption band 3400-3600 cm⁻¹, suggesting that both OH groups of the diol takes part in the esterification reaction. Similarly, other compounds **2b**, **2c**, **3b** and **3c** display characteristic IR peaks in the expected regions (Table 2).

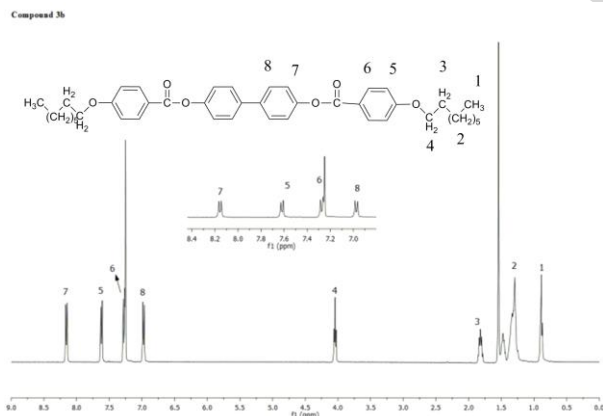
Table 2 Selected spectroscopic data (IR and ¹H NMR) for compounds **2a-c** and **3a-c**

Compounds	IR (cm ⁻¹)	¹ H NMR (ppm) ^a
2a	1707 (ν C=O, ester), 3458 (ν OH)	8.15 (d, 2H, biphenyl), 7.56 (d, 2H, biphenyl), 6.98 (d, 2H, biphenyl), 6.90 (d, 2H, biphenyl), 7.46 (d, 2H, aryl), 7.24 (d, 2H, aryl), 4.05 (t, 2H, OCH ₂), 1.78 (q, 2H, CH ₂), 1.5 (sx, 2H, CH ₂ -CH ₃), and 0.98 (t, 3H, CH ₃)
2b	1708 (ν C=O, ester), 3464 (ν OH)	8.16 (d, 2H, biphenyl), 7.56 (d, 2H, biphenyl), 6.98 (d, 2H, biphenyl), 6.89 (d, 2H, biphenyl), 7.45 (d, 2H, aryl), 7.24 (d, 2H, aryl), 4.04 (t, 2H, OCH ₂), 1.79 (q, 2H, CH ₂), 1.4 (sx, 2H, CH ₂ -CH ₃), and 0.85 (t, 3H, CH ₃)
2c	1730 (ν C=O, ester), 3331 (ν OH)	8.16 (d, 2H, biphenyl), 7.56 (d, 2H, biphenyl), 6.98 (d, 2H, biphenyl), 6.89 (d, 2H, biphenyl), 7.46 (d, 2H, aryl), 7.24 (d, 2H, aryl), 4.04 (t, 2H, OCH ₂), 1.79 (q, 2H, CH ₂), 1.57 (sx, 2H, CH ₂ -CH ₃), and 0.87 (t, 3H, CH ₃)
3a	1728 (ν C=O, ester)	8.17 (d, 2x2H, biphenyl), 6.99 (d, 2x2H, biphenyl), 7.63 (d, 2x2H, aryl), 7.29 (d, 2x2H, aryl), 4.06 (t, 2x2H, OCH ₂), 1.81 (q, 2x2H, CH ₂), 1.53 (sx, 2x18H, (CH ₂) ₉ -CH ₃), and 0.99 (t, 2x3H, CH ₃)
3b	1730 (ν C=O, ester)	8.17 (d, 2x2H, biphenyl), 6.96 (d, 2x2H, biphenyl), 7.63 (d, 2x2H, aryl), 7.29 (d, 2x2H, aryl), 4.04 (t, 2x2H, OCH ₂), 1.82 (q, 2x2H, CH ₂), 1.34 (sx, 2x18H, (CH ₂) ₉ -CH ₃), and 0.89 (t, 2x3H, CH ₃)
3c	1728 (ν C=O, ester)	8.17 (d, 2x2H, biphenyl), 6.99 (d, 2x2H, biphenyl), 7.63 (d, 2x2H, aryl), 7.29 (d, 2x2H, aryl), 4.04 (t, 2x2H, OCH ₂), 1.82 (q, 2x2H, CH ₂), 1.34 (sx, 2x18H, (CH ₂) ₉ -CH ₃), and 0.88 (t, 2x3H, CH ₃)

^a ¹H NMR spectra were referenced to 7.25 ppm (residual proton of CHCl₃) of CDCl₃.

Fig 1 ¹H NMR spectrum of compound **2b**

The ¹H NMR spectra of compound **2a-2c** and **3a-3c** could be fully assigned to the phenyl and alkyl proton resonances. The spectrum of **2b**, for example, displays two doublet resonances corresponding to the octyloxyphenyl ring, which are observed at 7.45 and 7.24 ppm, and four sets of doublet resonances corresponding to the biphenyl ring,

Fig 2 ¹H NMR spectrum of compound **3b**

which are observed at 8.16, 7.56, 6.98, 6.89 ppm. Additionally, the octyloxy alkyl protons are evident as triplet, quintet, septet and triplet resonances at 4.04, 1.79, 1.57 and 0.87 ppm, respectively (Table 2). Similar to **2b**, bis-benzoate **3b** displays two doublet resonances at 7.63 and 7.29 for the octyloxy phenyl protons. However, in contrast to **2b**, it exhibits two doublets at 8.17 and 6.99 ppm for the biphenyl ring confirming the symmetrical nature of biphenyl bis(benzoate) **3b**. Similarly, compounds **2a**, **2c** and **3a**, **3c** display peaks in the expected regions of the ¹H NMR spectra (Table 2). Representative ¹H NMR spectra of compound **2b** and **3b** are shown in Fig. 1 and 2, respectively. The aliphatic carbon skeletons, aromatic ring carbons and -C=O and OCH₂ functional groups of the mono- and bis-benzoate **2a-2c** and **3a-3c** could fully be characterized by the ¹³C NMR spectroscopy. The spectrum of **2b** displays a strong signal at 68.04 ppm due to the -

OCH₂ carbon and other carbons of the octyloxy group exhibit signals at 14.11, 22.67, 26.00, 29.12, 29.23, 29.34 and 31.82 ppm. The ester carbon displays signal at 165.23 ppm, and the phenyl and biphenyl ring carbons display signal at 114.35, 115.70, 121.51, 122.03, 127.72, 1228.37, 132.34, 133.15, 138.50, 150.05 and 155.27 ppm. Compared to the mono-benzoate **2b**, the bis-benzoate **3b** gives only eight signals in the aromatic region at 114.34, 121.51, 122.15, 128.18, 132.33, 138.11, 150.59 and 163.62 ppm, verifying the symmetrical nature of the compound as evident in the ¹H NMR spectrum.

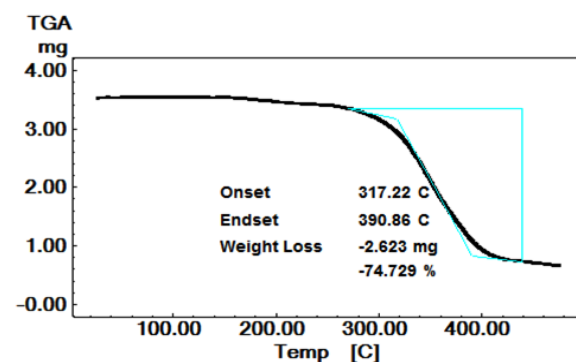
2.3. Thermal stability

Thermal studies of all compounds were performed by thermo gravimetric analysis (TGA) under nitrogen atmosphere. Analysis of the TG trace (heating rate 10 °C/min) shows that compound **2a-2c** and **2a-c** exhibit good thermal stability.

Table 3 Thermogravimetric data for **2a-c** and **3a-c**

Compounds	Decomposition onset (°C) on TGA	Decomposition endset (°C) on TGA	% of weight loss
2a	320	389	80
2b	332	402	75
2c	328	426	77
3a	375	428	65
3b	373	433	71
3c	360	419	62

Due to the presence of 4,4'-biphenyl aromatic ring based central core [26], the compounds exhibit high thermal stability, and decompositions are observed at ca. 320 °C for **2a**, 332 °C for **2b**, 328 °C for **2c**, 375 °C for **3a**, 373 °C for **3b**, and 360 °C for **3c** in the TG traces.

Fig. 3 TGA thermograms of compound **2a**

Representative TGA curve of compound **2a** is shown in Fig. 3. In mono-benzoate **2a-2c**, thermal stability slightly increases from **2a** to **2b** due to the increase of chain length of terminal moiety from OC₄H₉ to OC₈H₁₇, but decreases in **2c** for the further increase. The thermal stability of the bis-ester **3a-c** is higher than that of the monoester **2a-c** (Table 3), and in the series, thermal stability decreases with increase of the chain length of the terminal moiety (Table

3). Among the ester compounds, the highest thermal stability is observed for **3a** (decomposition onset at 375 °C). The weight loss (77-80%) in mono-benzoate is much higher than that of bis-benzoate (62-65%).

2.4. Phase clarifications of compounds **2** and **3**

The phase behavior of compounds **2a-c** and **3a-c** were investigated by a combination of DSC (Fig 4) and POM (Fig. 6-11). DSC traces of compounds **2** and **3** predict the existence of liquid crystal phases. The phase transition temperatures observed with DSC are consistent with those detected by POM. The mesophase type and phase transition temperatures are summarized in Table 4. The DSC thermogram of **3c** is shown in Fig. 4. In POM, all the compounds exhibit strong birefringences characteristic of liquid crystalline behavior during the heating and cooling.

2.4.1 Mono-benzoate **2a-2c**

Compound **2a**, on second heating, exhibits crystal to mesophase transition at 204.9 °C with enthalpy change of 73.7 J/g, and mesophase to isotropic liquid transition at 239.9 °C with enthalpy change of 2.1 J/g. POM of the compound displays thread-like textures of an enantiotropic nematic mesophase. DSC shows that it has a glass transition at 121.8 °C during the first heating, which is lost in the second heating.

Table 4 Phase transition temperatures and enthalpies change of compounds **2a-c** and **3a-c**

Compounds	Heating cycle ^a	Cooling cycle ^a
2a	Cr-N 204.9 (73.7), N-IL 239.9 (2.1)	IL-N 262.1 (0.5), N-Cr 131.5 (39.7)
2b	Cr ₁ -Cr ₂ 111.5 (4.9), Cr-N 177.2 (77.1), N-IL 198.7 (5.1)	IL-N 219.9 (1.6), N- SmA 143.3 (35.1), SmA-Cr 120.6 (10.3)
2c	Cr-SmA 97.7 (19.4), SmA-IL 155.4 (28)	IL-SmA 157.5 (33.3), SmA-Cr 93.9 (22.9)
3a	Cr-SmA 151.7, (26.5), SmA-N 178.0 (44.2), N-IL 360.4 (6.3)	IL-N 362.1 (6.6), N- SmA 169.4 (40.6), SmA-Cr 116.4 (4.6)
3b	Cr ₁ -Cr ₂ 109.0 (7.1), Cr ₂ -SmA 140.0 (39.5), SmA-N 212.9 (4.0), N-IL 290.3 (3.5)	IL-N 292.4 (2.9), N- SmA 213.8 (3.7), SmA- SmC 138.5 (18.7), SmC-Cr 125.8 (11.0)
3c	Cr ₁ -Cr ₂ 71.6 (11.1), Cr-SmC 115.5 (30.3), SmC-SmA 125.2 (16.7), SmA-N 220.1 (4.9), N-IL 245.8 (1.3)	IL-N 249.5 (1.5), N- SmA 229.3 (3.9), SmA- SmC 127.6 (16.5), SmC-Cr 96.4 (36.4), Cr ₂ -Cr ₁ 63.9 (3.0)

^a Enthalpy change ($\Delta H/Jg^{-1}$) given in bracket. Cr = Crystalline phase, N = Nematic phase, IL = Isotropic Liquid, Sm A = Smectic A phase, Sm C = Smectic C phase.

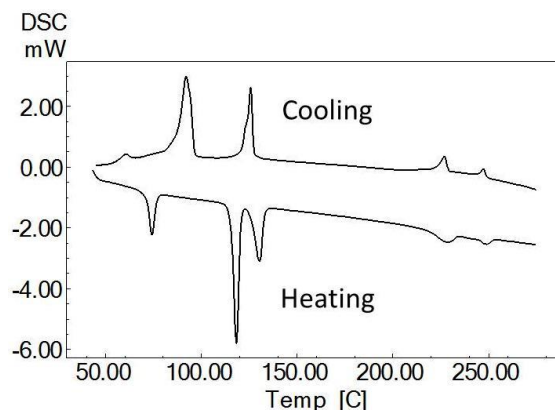


Fig. 4 DSC thermogram (10 °C/min heating/cooling) of **3c**

Compound **2b**, with longer alkoxy chain (OC₈H₁₇) than **2a** (OC₄H₉), on heating, shows a glass transition at 86.3 °C, a crystal to crystal transition at 111.5 °C and a nematic transition at 177.2 °C. On slow cooling it displays an additional smectic A (Sm A) transition at 143.3 °C. The nematic droplets of the nematic phase and batonnet texture of the Sm A phase are observed on POM (Fig. 6). Compound **2c**, with the longest alkoxy chain (OC₁₂H₂₅), exhibits only smectic A mesophase. POM demonstrates batonnet textures, both on heating and cooling, which is characteristic to Sm A phase (Fig. 7). In the hydroxyl mono-benzoate series **2a-2c**, the length of the alkoxy chain is varied keeping the core aromatic structure same, and it is observed in the DSC that the melting point as well as nematic phase stability decreases from **2a** to **2b** with increase of chain length. The nematic ranges for **2a** and **2b** are 21.5 °C and 35 °C, respectively; it also decreases with increase of chain length (Fig. 5). The longest alkoxy chain (OC₁₂H₂₅) in **2c**, compared to **2a** and **2b**, dictates the mesophase to be smectic [27].

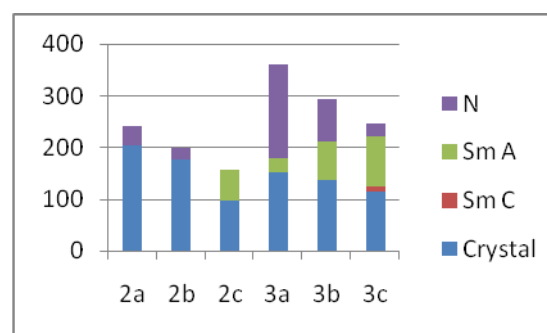


Fig. 5 Phase temperature ranges of **2a-2c** and **3a-3c** during heating

2.4.2 Bis-benzoate **3a-3c**

Compound **3a** (OC₄H₉ terminal moiety) exhibits three endothermic and three exothermic transitions as evident by DSC (Table 4). POM shows enantiotropic nematic and smectic A mesophases during heating and cooling. The phases are reflected by schlieren texture (nematic) and

feather like texture (Sm A) (Fig. 8). Similarly, **3b**, on heating, displays Sm A and nematic mesophases (Fig. 9). However, it exhibits an additional Sm C phase during cooling. Compared to **3a** and **3b**, **3c** exhibits enantiotropic Sm C, Sm A (Fig. 10) and nematic transitions. The Sm C, Sm A and nematic phases are reflected by broken focal conic, focal conic and schlieren textures, respectively. The new bis-benzoates **3a-3c** are symmetrical molecules where the central biphenyl core, in its 4,4' position, is linked to an additional phenyl ring through ester linkage, thus increases the length to breadth ratio of the molecules. With shorter alkoxy chain, **3a** shows the nematic stability 362.1 °C with largest nematic range (182.4 °C) of the series (Fig. 5). With short alkoxy chain (OC₄H₉), it also shows smectic phase with narrow range probably due to the lateral attraction for the resultant dipole of ester bridged aromatic rings [26-27]. As the terminal chain length increases from C₄ to C₈, the melting point and nematic phase stability of **3b** decreases, but the smectic A phase stability increases, as expected (Fig. 5). In **3c**, with the OC₁₂H₂₅ terminal moiety, an additional smectic C phase (Fig. 5) is observed because of lamellar packing which is stabilized by the longest (C₁₂) terminal chain [26-28]. While n-alkyl and n-alkoxy cyanobiphenyl are commercially important mesogens [29], and their thermally stable analogues are used in designing polymer composites [30], the hydroxy functionalized analogues are used as pendant cores in side chain LC polymers [31].

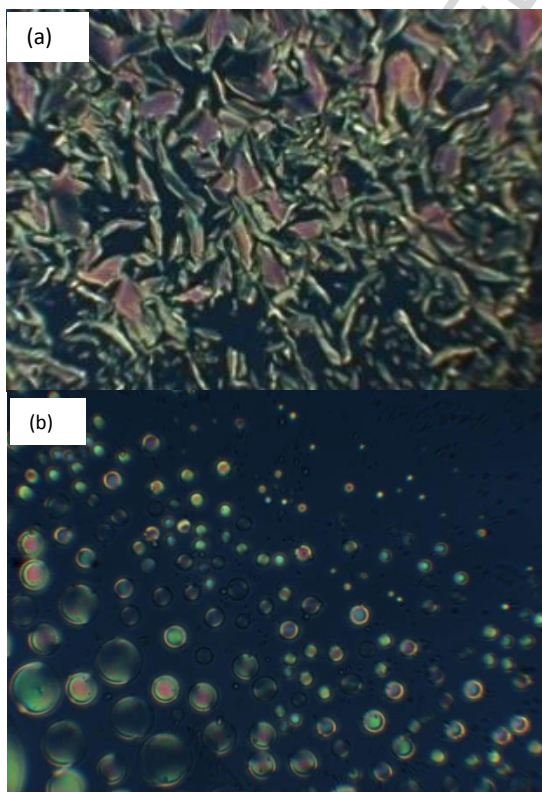


Fig. 6 Optical texture of **2b**. Batonnet texture (a) of smectic A phase at 125.3 °C, and nematic droplets (b) of nematic phase at 219.0 °C

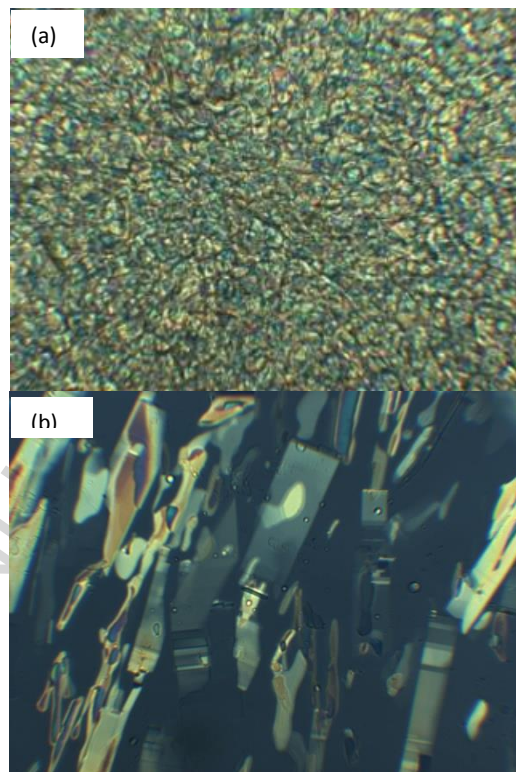


Fig. 7 Optical texture of **2c**. Batonnet textures of smectic A phase at 168.7 °C during heating (a), and at 165.3 °C (b) during cooling.

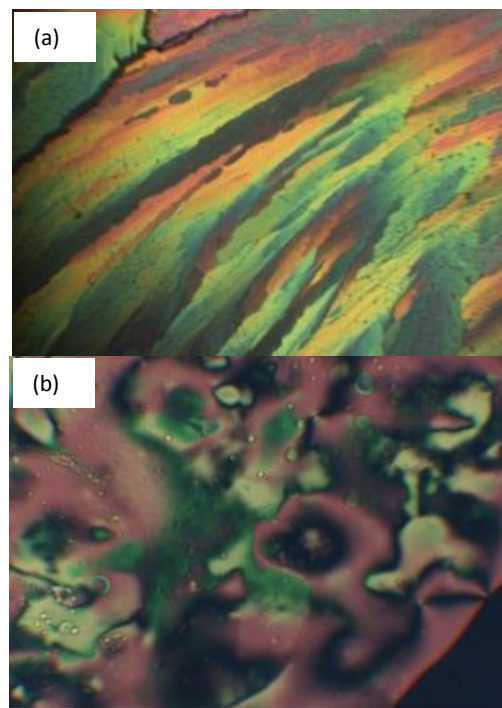


Fig. 8 Optical texture of **3a**. Feather like texture (a) of smectic A phase at 145.4 °C, and (b) schlieren texture of nematic phase at 305.4 °C

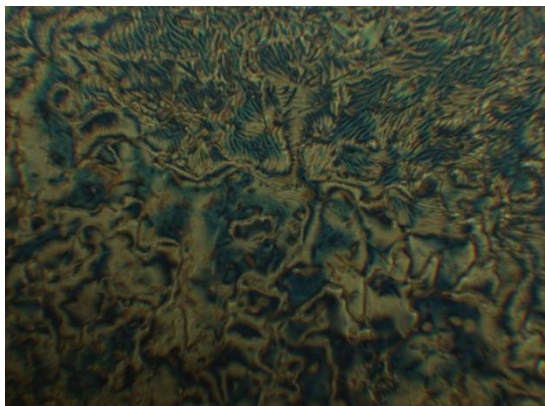


Fig. 9 Optical texture of **3b**. Thread like texture of nematic phase at 210.3 °C

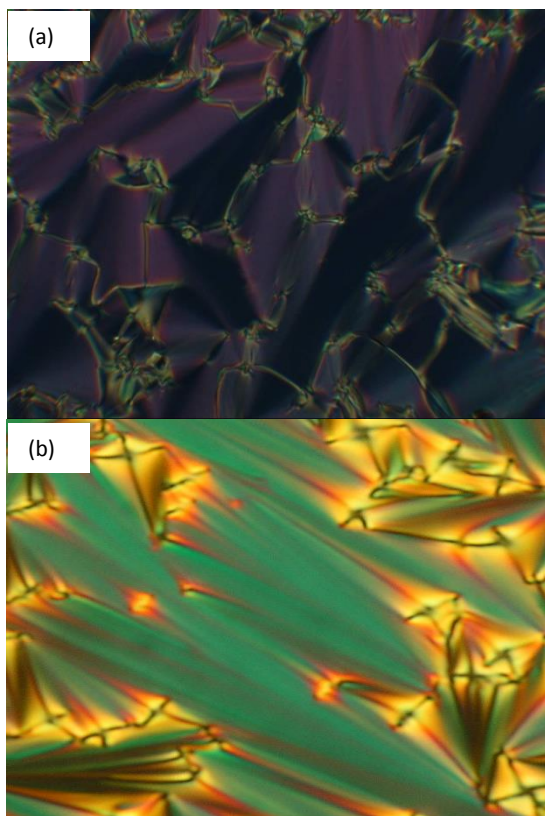


Fig. 10 Optical texture of **3c**. Broken focal conic texture (a) of smectic C phase at 122.6 °C, and focal conic texture (b) of smectic A phase at 125.19 °C

3.3 Chiral domains of **3a-3c**

POM demonstrates that though compound **3a-3c** has no chiral center of its own, it shows chirality under the microscope with respect to the alignment of polarizer and analyzer due to the tilting of molecules or the helical arrangement of one group of molecules with respect to another. When the samples are observed under slightly

uncrossed polarizer, the texture is split into darker and brighter domains, and by uncrossing the polarizer in opposite directions by the same angle, the darker and brighter domains are exchanged (Fig. 11), indicating that the domains are twisted in opposite directions [20a,d]. The chirality of a twist-bend nematic phase, formed by methylene link, can be identified by NMR spectroscopy [32]. Achiral nematic liquid crystal 5CB can be used to create template blue phases that can act as mirrorless laser and switchable opto-electronic devices [33].

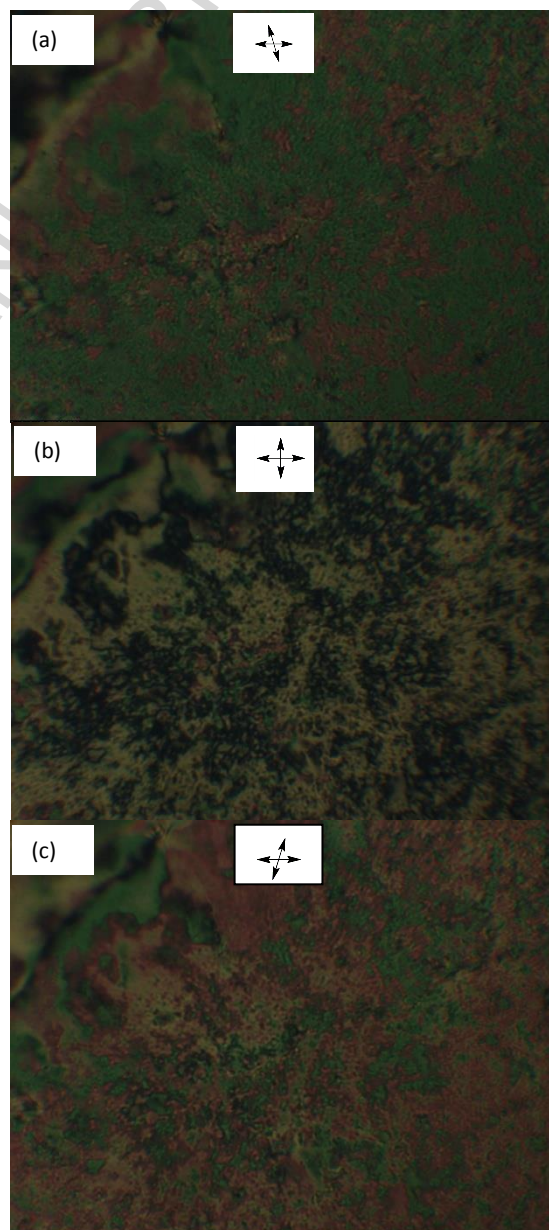


Fig. 11 Optical texture of **3b** under uncrossed and crossed polarizer at 295 °C. Domains of opposite handed optical activity upon decrossing the analyzer relative to the polarizer, to the left (a), to the right (c). DC phase appears as dark between crossed polarizer (b).

2.5. Absorption and emission properties of the compounds

The investigation of UV/Vis absorption spectroscopy of all the compounds was carried out at room temperature. The lowest energy absorption bands in the UV/Vis spectra, in chloroform solution, at room temperature, for compounds **2a-c**, (1.25×10^{-5} mol/L for **2a** and **2c**, and 1.11×10^{-5} mol/L for **2b**) are observed at 269 nm, and that for compounds **3a-c** (1.25×10^{-5} mol/L for **3a**, 1.11×10^{-5} mol/L for **3b** and 1.0×10^{-5} mol/L **3c**) are also observed at the same peak position (Fig. 12). The variation of alkoxy substituent (butoxy, octyloxy, and dodecyloxy) in compounds **2a-c** and **3a-c** has no effect in absorption maxima. By comparing with the related systems, the lowest energy band, in each case, is attributed to the absorption at the 1,4-biphenyl core [34]. The photoluminescence spectrum of **2** and **3** displays emission bands in the ultraviolet to violet region (Fig. 12). The room temperature spectral measurement of compounds **2a-c** and **3a-c**, recorded in chloroform under excitation at the wavelength of the absorption maximum ($\lambda_{\text{max}} = 269$ nm), shows emission maxima at 336 nm for **2a-c**, and at 380 nm, 362 nm and 353 nm, for compounds **3a**, **3b** and **3c**, respectively. The optical (absorption and emission) properties of some related systems [34] have been reported recently.

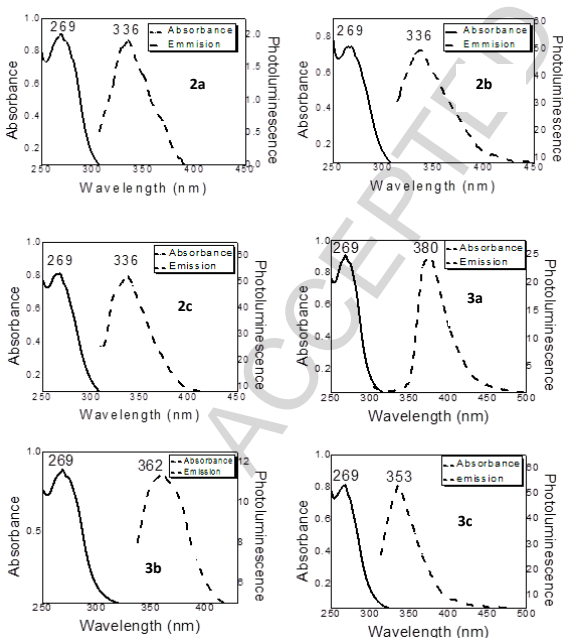


Fig. 12 Absorption and emission spectra of **2a-c** and **3a-c**

2.6. Theoretical Studies

The origin of the electronic transitions in the target compounds were analyzed computationally taking **2a** and **3a** as the representative compounds. The geometries of the compounds were optimized at B3LYP [35] density functional level with 6-31++g(d,p) basis set. All calculations were performed with GAUSSIAN 03 package on BRAF supercomputing environment.

The theoretical electronic transitions for the compounds are presented in Table 5. The results indicate the major and minor contributors involved in the transition. Interestingly, for the compound **3a**, the major contributor is not HOMO->LUMO; rather the orbitals H-2 to L+2 are involved in the transition. The density of states (DOS) profile (Fig. 13B) indicates the presence of two sets of closely packed energy levels for the compound **3a**. Such densely spaced orbitals may be responsible for the involvement of orbitals higher (and lower) than the frontier orbitals in the transition of electron. Another important feature is the nature of frontier orbitals. For **3a**, both the HOMO and LUMO are centered at the terminal aromatic unit, but for the compound **2a**, the HOMO is centered far away at the central aromatic unit, which in turn is probably responsible for the difference in DOS.

Table 5 Contributors responsible for the electronic transitions

Compounds	Absorption maxima (nm)		Contributors
	Expt	Theo	
2a	269	232	HOMO->LUMO (19%) HOMO->L+1 (68%) H-5->L+7 (2%) H-2->L+4 (3%) H-1->L+2 (6%)
3a	269	218	H-2->LUMO (22%) H-1->L+1 (35%) HOMO->L+2 (21%) H-7->L+7 (4%) H-6->L+5 (7%) H-5->L+4 (5%)

3. Experimental details

3.1. Materials and techniques

Solvents were dried, distilled from appropriate drying agents and degassed before use [36]. The compounds $\text{H}_9\text{C}_4\text{O}-\text{C}_6\text{H}_4-\text{COOH}$ [37], $\text{H}_{17}\text{C}_8\text{O}-\text{C}_6\text{H}_4-\text{COOH}$ [37] and $\text{H}_{25}\text{C}_{12}\text{O}-\text{C}_6\text{H}_4-\text{COOH}$ [37] were prepared by literature methods. NMR spectra were recorded on Bruker 400 MHz NMR spectrometer in CDCl_3 solvent. ^1H and ^{13}C NMR spectra were referenced to solvents resonances. Infrared spectra were recorded on Shimadzu Prestige 21 FTIR spectrometer by using KBr pellets or solution in dichloromethane. The thermal stability was assessed with a Shimadzu TGA-50 thermogravimetric analyzer under nitrogen atmosphere. Samples were heated in the range from 25 °C to 500 °C, at heating rate of 10 °C/min, in an aluminium crucible. The phase transition temperatures and associated enthalpies were recorded using differential scanning calorimeter (DSC) with a Shimadzu TA-60A instrument, at a heating/cooling rate of 10 °C/min, under nitrogen atmosphere. Samples were heated in the range from 25 °C to 350 °C, in an aluminium crucible.

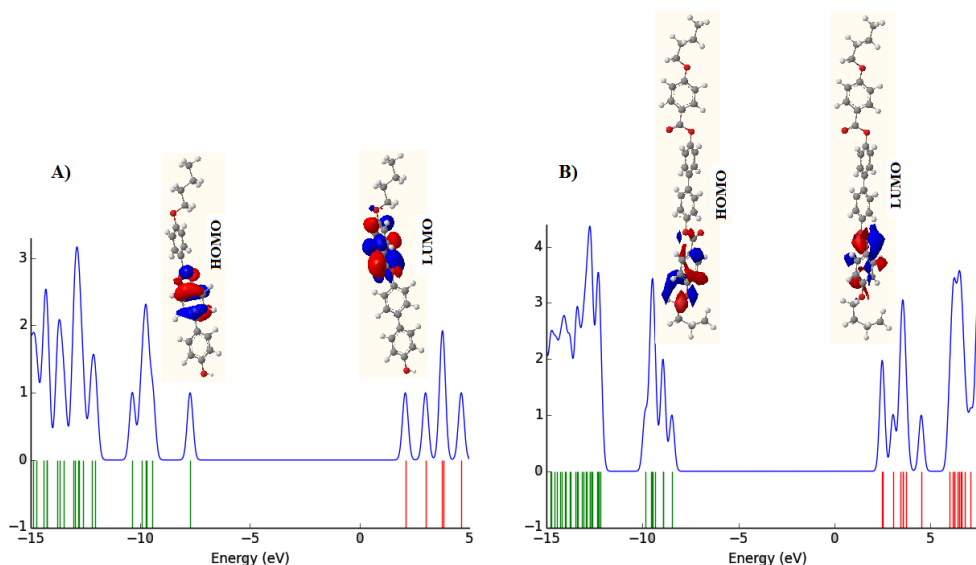


Fig. 13 Density of States (DOS) profile showing HOMO and LUMO for the compounds **2a** (A) and **3a** (B)

The mesophases exhibited by the hydroxybiphenyl alkoxybenzoate **2a-c** and biphenyl bis(alkoxybenzoate) **3a-c** were observed and characterized by using a Olympus TH4-200 microscope equipped with a Linkam hot stage and temperature controller (H95-HS).

3.2. Syntheses

3.2.1. 4'-Hydroxy-[1,1'-biphenyl]-4-yl 4-(butoxy)benzoate (**2a**) and [1,1'-biphenyl]-4,4'-diyl bis(4-(butoxy)benzoate) (**3a**)

A mixture of 4-butoxybenzoic acid (**1a**) (0.45 g, 2.32 mmol) and 1,1'-biphenyl-4,4'-diol (0.432 g, 2.32 mmol) in presence of dicyclohexylcarbodiimide (DCC) (0.478 g, 2.32 mmol) and dimethylaminopyridine (DMAP) (0.283 g, 2.32 mmol) in dichloromethane (20 mL) was degassed under nitrogen atmosphere and the resulting mixture was stirred for 24 hours at room temperature. After completion the reaction, the precipitate was removed by filtration. The solvent was removed in under reduced pressure, and the solid residue was redissolved in dichloromethane and the undissolved solid was removed by filtration. Then, the resulting solution was washed with 10% cold acetic acid followed by brine solution, and dried over anhydrous magnesium sulfate. After that, the solvent was removed under reduced pressure, and the solid residue was purified by column chromatography on silica gel eluting with hexane and dichloromethane (2:1). The first band was separated and identified as **3a**, and the second band as **2a**, as white solids, in 18.34% (0.228 g) and 21.50% (0.18 g) yield, respectively. **2a**: IR (solid state, KBr): ν 3458 (-OH), 1707 (-CO-, ester) cm^{-1} ; ^1H NMR (400 MHz, CDCl_3): δ 8.15 (d, 2H, biphenyl), 7.56 (d, 2H, biphenyl), 7.46 (d, 2H, aryl), 7.24 (d, 2H, aryl), 6.98 (d, 2H, biphenyl), 6.90 (d, 2H, biphenyl), 4.05 (t, 2H, OCH_2), 1.78 (q, 2H, CH_2), 1.5 (sx, 2H, $\text{CH}_2\text{-CH}_3$), and 0.98 (t, 3H, CH_3); ^{13}C NMR (100

MHz, CDCl_3): δ 13.83, 19.21, 31.12, 68.04, 114.33, 115.70, 121.51, 122.03, 127.72, 128.39, 132.32, 133.27, 138.37, 150.05, 155.28, 163.59, and 165.23; Anal. Calc. for $\text{C}_{23}\text{H}_{22}\text{O}_4$: C, 76.22; H, 6.12%. Found: C, 76.30; H, 6.15%. **3a**: IR (solid state, KBr): ν 1728 (-CO-, ester) cm^{-1} ; ^1H NMR (400 MHz, CDCl_3): δ 8.17 (d, 2 \times 2H, biphenyl), 7.63 (d, 2 \times 2H, aryl), 7.29 (d, 2 \times 2H, aryl), 6.99 (d, 2 \times 2H, biphenyl), 4.06 (t, 2 \times 2H, OCH_2), 1.81 (q, 2 \times 2H, CH_2), 1.53 (sx, 2 \times 2H, $\text{CH}_2\text{-CH}_3$), and 0.99 (t, 2 \times 3H, CH_3); ^{13}C NMR (100 MHz, CDCl_3): δ 13.83, 19.22, 31.16, 68.05, 114.34, 121.52, 122.15, 128.18, 132.34, 138.11, 150.59, 163.62, and 165.01; Anal. Calc. for $\text{C}_{34}\text{H}_{34}\text{O}_6$: C, 75.82; H, 6.36%. Found: C, 75.71; H, 5.87%.

3.2.2. 4'-Hydroxy-[1,1'-biphenyl]-4-yl 4-(octyloxy)benzoate (**2b**) and [1,1'-biphenyl]-4,4'-diyl bis(4-(octyloxy)benzoate) (**3b**)

The same procedure as for compound **2a** and **3a** was followed for the synthesis of **2b** and **3b**, but 4-octyloxybenzoic acid **1b**, was used instead of 4-butoxybenzoic acid, **1a**. Yield: **3b** 25.5%; **2b** 24.6%.

2b: IR (solid state, KBr): ν 3464 (-OH), 1708 (-CO-, ester) cm^{-1} ; ^1H NMR (400 MHz, CDCl_3): δ 8.16 (d, 2H, biphenyl), 7.56 (d, 2H, biphenyl), 7.45 (d, 2H, aryl), 7.24 (d, 2H, aryl), 6.98 (d, 2H, biphenyl), 6.89 (d, 2H, biphenyl), 4.9 (s, 1H, -OH), 4.04 (t, 2H, OCH_2), 1.79 (q, 2H, CH_2), 1.4 (m, 10H, $(\text{CH}_2)_5\text{-CH}_3$), and 0.85 (t, 3H, CH_3); ^{13}C NMR (100 MHz, CDCl_3): δ 14.11, 22.67, 26.00, 29.12, 29.23, 29.34, 31.82, 68.38, 114.35, 115.70, 121.51, 122.03, 127.72, 128.37, 132.34, 133.15, 138.50, 150.05, 155.27, 163.62, and 165.23; Anal. Calc. for $\text{C}_{27}\text{H}_{30}\text{O}_4$: C, 77.48; H, 7.22%. Found: C, 77.12; H, 6.69%. **3b**: IR (solid state, KBr): ν 1730 (-CO-, ester) cm^{-1} ; ^1H NMR (400 MHz, CDCl_3): δ 8.17 (d, 2 \times 2H, biphenyl), 7.63 (d, 2 \times 2H, aryl), 7.29 (d, 2 \times 2H, aryl), 6.96 (d, 2 \times 2H, biphenyl), 4.04 (t, 2 \times 2H, OCH_2), 1.82 (q, 2 \times 2H, CH_2), 1.34 (m, 2 \times 10H, $(\text{CH}_2)_5\text{-CH}_3$), and 0.89 (t, 2 \times 3H, CH_3); ^{13}C NMR (100

MHz, CDCl₃): δ 14.11, 22.67, 26.01, 29.12, 29.24, 29.34, 31.82, 68.37, 114.34, 121.51, 122.15, 128.18, 132.33, 138.11, 150.59, 163.62, and 165.01; Anal. Calc. for C₄₂H₅₀O₆: C, 77.51; H, 7.74%. Found: C, 77.55; H, 7.32%.

3.2.3. 4'-Hydroxy-[1,1'-biphenyl]-4-yl 4-(dodecyloxy) benzoate (**2c**) and [1,1'-biphenyl]-4,4'-diyl bis{4-(dodecyloxy)benzoate} (**3c**)

The same procedure as for compound **2a** and **3a** was applied for the synthesis of **2c** and **3c**, but 4-dodecyloxybenzoic acid **1c**, was used instead of 4-butoxybenzoic acid, **1a**. Yield: **3c** 14.2%; **2c** 20.7%.

2c: IR (solid state, KBr): ν 3331 (-OH), 1730 (-CO-, ester) cm⁻¹; ¹H NMR (400 MHz, CDCl₃): δ 8.16 (d, 2H, biphenyl), 7.56 (d, 2H, biphenyl), 7.46 (d, 2H, aryl), 7.24 (d, 2H, aryl), 6.98 (d, 2H, biphenyl), 6.89 (d, 2H, biphenyl), 4.04 (t, 2H, OCH₂), 1.79 (q, 2H, CH₂), 1.57 (m, 18H, (CH₂)₉-CH₃), and 0.87 (t, 3H, CH₃-); ¹³C NMR (100 MHz, CDCl₃): δ 14.13, 22.70, 25.99, 29.12, 29.36, 29.37, 29.57, 29.60, 29.64, 29.67, 31.93, 68.37, 114.33, 115.70, 121.51, 122.02, 127.71, 128.37, 132.22, 133.19, 138.37, 150.05, 155.28, 163.62, and 165.23; Anal. Calc. for C₃₁H₃₈O₄: C, 78.45; H, 8.07%. Found: C, 78.17; H, 7.18%. **3c**: IR (solid state, KBr): ν 1728 (-CO-, ester) cm⁻¹; ¹H NMR (400 MHz, CDCl₃): δ 8.17 (d, 2 \times 2H, biphenyl), 7.63 (d, 2 \times 2H, aryl), 7.29 (d, 2 \times 2H, aryl), 6.99 (d, 2 \times 2H, biphenyl), 4.04 (t, 2 \times 2H, OCH₂), 1.82 (q, 2 \times 2H, CH₂), 1.34 (m, 2 \times 18H, (CH₂)₉-CH₃), and 0.88 (t, 2 \times 3H, CH₃-); ¹³C NMR (100 MHz, CDCl₃): δ 14.11, 22.70, 26.00, 29.12, 29.36, 29.38, 29.57, 29.60, 29.65, 29.67, 31.93, 68.37, 114.34, 121.51, 122.15, 128.18, 132.33, 138.11, 150.59, 163.62, and 165.01; Anal. Calc. for C₅₀H₆₆O₆: C, 78.70; H, 8.72%. Found: C, 78.58; H, 8.36%.

4. Conclusions

A series of hydroxybiphenyl 4-alkoxybenzoate and biphenyl bis-(4-alkoxybenzoate) have been synthesized successfully by esterification reaction. The newly formed compounds are fully characterized by spectroscopic and analytical techniques. All the synthesized compounds exhibit good thermal stability, higher than 300 °C, as evident by the thermo gravimetric analysis. The synthesized ester products exhibit liquid crystalline properties which are confirmed by the phase transitions on differential scanning calorimetry (DSC) and texture behaviors on polarizing optical microscope (POM). All mono-benzoates with shorter alkoxy chain, OC₄H₉ and OC₈H₁₇ exhibit nematic mesophase, and that with longer carbon chain, OC₁₂H₂₅ exhibits smectic phase. Bis-benzoates exhibit both nematic and smectic mesophases. With increasing carbon chain length nematic phase stability decreases, and bis-benzoate with OC₁₂H₂₅ possesses nematic, smectic A and smectic C phases. The POM images demonstrate that though the bis-benzoates have no chiral center of their own, they exhibit chirality under microscope with respect to the alignment of polarizer and analyzer, due to the helical arrangement of one group of molecules with respect to another. Computational study of

compounds **2a** and **3a** were performed with GAUSSIAN 03 package as representative compounds.

Acknowledgements

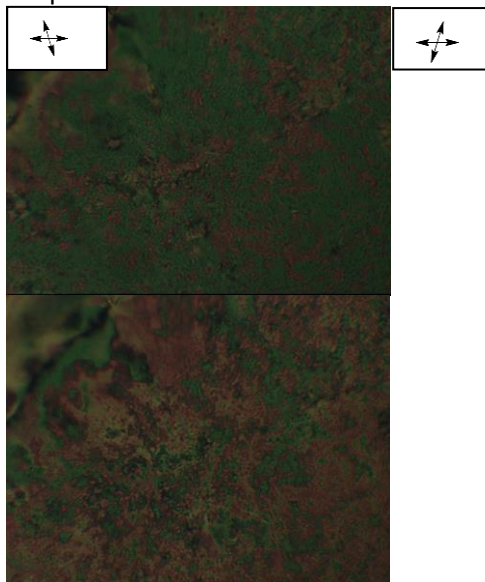
We acknowledge Higher Education Quality Enhancement Project (HEQEP) (CP 2524) of University Grants Commission of Bangladesh for funding.

References

1. A. Seeboth, and D. Löttsch, *Thermochromic and Thermotropic Materials*, Pan Stanford, Singapore, 2014.
2. (a) R.P. Lemieux, *Acc. Chem. Res.* 34 (2001) 845; (b) A. Saha, Y. Tanaka, Y. Han, C.M.W. Bastiaansen, D.J. Broer, R.P. Sijbesma, *Chem. Commun.* (2012) 4579.
3. (a) I. Sage, *Liq. Cryst.* 38 (2011) 1551; (b) M. O'Neill, S.M. Kelly, *Adv. Mater.* 23 (2011) 566; (c) M.P. Aldred, A.E.A. Contoret, S.R. Farrar, M.K. Stephen, D. Mathieson, M. O'Neill, W.C. Tsoi, P. Vlachos, *Adv. Mater.* 17 (2005) 1368.
4. H.K. Bisoyi, Q. Li, *Acc. Chem. Res.* 47 (2014) 3184.
5. C. Ohm, M. Drehmer, R. Zentel, *Adv. Mater.* 22 (2010) 3366.
6. Y. Wang, Q. Li, *Adv. Mater.* 24 (2012) 1926.
7. D.J. Mulder, A.P.H.J. Schenning, C.W.M. Bastiaansen, *J. Mater. Chem. C* 2 (2014) 6695.
8. N. Tamaoki, *Adv. Mater.* 13 (2001) 1135.
9. (a) M. Frogoli, G.H. Mehl, *Chem. Phys. Chem.* 1 (2003) 101; (b) M. Irie, *Chem. Rev.* 100 (2000) 1685.
10. D.M. Walba, *Science* 270 (1995) 250.
11. J.W. Goodby, R. Blinc, N.A. Clark, S.T. Lagerwall, M.A. Osipov, S.A. Pikin, T. Sakurai, K. Yoshino, B. Zeks in *Ferroelectricity and Related Phenomena*, Vol. 7, ed. George Taylor, Gordon and Breach, Philadelphia, 1992.
12. Y. Wang, A. Urbas, Q. Li, *J. Am. Chem. Soc.* 134 (2012) 3342.
13. (a) H.S. Kitzerow, C. Bahr, *Chirality in Liquid Crystals*, Springer, New York, 2000; (b) S. Pieraccini, S. Masiero, A. Ferrarini, G.P. Spada, *Chem. Soc. Rev.* 40 (2011) 258; (c) J.W. Goodby, *J. Mater. Chem.* 1 (1991) 307.
14. Z. Zheng, Y. Li, H.K. Bisoyi, L. Wang, T.J. Bunning, Q. Li, *Nature* 531 (2016) 352.
15. R.P. Lemieux, *Chem. Soc. Rev.* 36 (2007) 2033.

16. (a) D. Coates, G.W. Gray, *Phys. Lett. A* 45 (1973) 115; (b) M. Lee, S.T. Hur, H. Higuchi, K. Song, S.W. Choi, H. Kikuchi, *J. Mater. Chem.* 20 (2010) 5813.
17. (a) H.J. Coles, M.N. Pivnenko, *Nature* 436 (2005) 997; (b) H. Kikuchi, M. Yokota, Y. Hisakado, H. Yang, T. Kajiyama, *Nat. Mater.* 1 (2002) 64.
18. (a) S.R. Renn, T.C. Lubensky, *Phys. Rev. A* 38 (1988) 2132; (b) J.W. Goodby, M.A. Waugh, S.M. Stein, E. Chin, R. Pindak, J.S. Patel, *Nature* 337 (1989) 449; (c) G. Srajer, R. Pindak, M.A. Waugh, J.W. Goodby, J.S. Patel, *Phys. Rev. Lett.* 64 (1990) 1545.
19. (a) S. Pieraccini, S. Masiero, A. Ferrarini, G. P. Spada, *Chem. Soc. Rev.*, 40 (2011) 258; (b) R. P. Lemieux, *Acc. Chem. Res* 34 (2001) 845.
20. (a) H. Sasaki, Y. Takanishi, J. Yamamoto, A. Yoshizawa, *Soft Matter* 12 (2016) 3331; (b) V. Borshch, Y.-K. Kim, J. Xiang, M. Gao, A. Jakli, V. P. Panov, J.K. Vij, C.T. Imrie, M.G. Tamba, G.H. Mehl, O.D. Lavrentovich, *Nat. Commun.* 4 (2013) 2635; (c) L.E. Hough, M. Spanuth, M. Nakata, D.A. Coleman, C.D. Jones, G. Dantlgraber, C. Tschierske, J. Watanabe, E. Korblova, D.M. Walba, J.E. MacLennan, M.A. Glaser, N.A. Clark, *Science* 325 (2009) 452; (d) A. Jakli, *Liq. Cryst. Rev.* 1 (2013) 65.
21. (a) H. Takezoe, Y. Takanishi, *Jpn. J. Appl. Phys.* 45 (2006) 597; (b) R. A. Reddy, C. Tschierske, *J. Mater. Chem.* 16 (2006) 907.
22. (a) J.W.Y. Lam, X. Kong, Y. Dong, K.K.L. Cheuk, K. Xu, B.Z. Tang, *Macromolecules* 33 (2000) 5027; (b) V. Percec, A.D. Asandei, D.H. Hill, D. Crawford, *Macromolecules* 32 (1999) 2597.
23. K. Goossens, K. Lava, P. Nockemann, K.V. Hecke, L. V. Meervelt, P. Pattison, K. Binnemans, and T. Cardinaels, *Langmuir* 25 (2009) 5881.
24. J. Wang, Y. H. Wang, *Chin. Chem. Lett.* 19 (2008) 359.
25. R.M. Silverstein, G.C. Bassler, T.C. Morrill, *Spectroscopic Identification of Organic Compounds*, John Wiley and Sons, Singapore, 1991.
26. T. Ranganathan, C. Remashand A. Kumar, *Liq. Cryst.* 32 (2005) 499.
27. P.T. Colling, M. Hird, *Introduction to Liquid Crystals: Physics and Chemistry*, Taylor and Francis, London, 1997.
28. A.J. Eagle, T.M. Herrington, N.S. Isaacs, *Liq. Cryst.* 24 (1998) 735.
29. G.W. Gray, *Molecular Structure and the Properties of Liquid Crystals*. Academic Press, London, 1962.
30. K.-S. Jang, J.C. Johnson, T. Hegmann, E. Hegmann, L.T.J. Korley, *Liq. Cryst.* 14 (2014) 1473.
31. (a) R.P. Nieuwhof, A.T.M. Marcelis, J.R. Sudhölter, S.J. Picken, W.H. de Jeu, *Macromolecules* 32 (1999) 1398; (b) B. Z. Tang, X. Kong, X. Wan, H. Peng, and W. Y. Lam, *Macromolecules* 31 (1998) 2419; (c) S.-H. Yang, C.-S. Hsu, *J. Polym. Sci., Part A: Polym. Chem.* 47 (2009) 2713.
32. J.W. Emsley, M. Lelli, A. Lesage, G. R. Luckhurst, B.A. Timimi, H. Zimmermann, *J. Phys. Chem. B* 116 (2012) 7940.
33. F. Castles, F.V. Day, S.M. Morris, D-H. Ko, D.J. Gardiner, M. M. Qasim, S. Nosheen, P.J.W. Hands, S.S. Choi, R.H. Friend, H.J. Coles, *Nat. Mater.* 11 (2012) 599.
34. (a) T. Mori and M. Kijima, *Mol. Cryst. Liq. Cryst.* 489 (2008) 246; (b) E-J. Choi, F. Xu, *Mol. Cryst. Liq. Cryst.* 529 (2010) 147.
35. A.D. Becke, *J. Chem. Phys.* 98 (1993) 5648.
36. W.L.F. Armarego, D.D. Perrin, *Purification of Laboratory Chemicals*, 4th ed. Butterworth-Heinemann, Guildford, 1996.
37. J. Jensen, S.C. Grundy, S.L. Bretz, C.S. Hartley, *J. Chem. Edu.* 88 (2011) 1133.

Graphical Abstract



Chirality is observed in achiral biphenyl bis-benzoates as evident by optical textures under uncrossed ($< 20^\circ$) optical polarizer

Highlights

- Synthesis and spectroscopic characterization of a series of biphenyl mono- and bis-benzoates
- Biphenyl benzoates exhibit excellent thermal stability
- Chiral domains are observed in achiral biphenyl bis-benzoates

ACCEPTED MANUSCRIPT